Forces and conservation laws for motion on our spheroidal Earth

Boyd F. Edwards, and John M. Edwards

Forces and conservation laws for motion on our spheroidal Earth

Boyd F. Edwards[a)]
Department of Physics, Utah State University, Logan, Utah 84322

John M. Edwards
Department of Computer Science, Utah State University, Logan, Utah 84322

We explore the forces and conservation laws that govern the motion of a hockey puck that slides without friction on a smooth, rotating, self-gravitating spheroid. The earth's oblate spheroidal shape (apart from small-scale surface features) is determined by balancing the gravitational forces that hold it together against the centrifugal forces that try to tear it apart. The earth achieves this shape when the apparent gravitational force on the puck, defined as the vector sum of the gravitational and centrifugal forces, is perpendicular to the earth's surface at every point on the surface. Thus, the earth's spheroidal deformations neutralize the centrifugal and gravitational forces on the puck, leaving only the Coriolis force to govern its motion. Motion on the spheroid therefore differs profoundly from motion on a rotating sphere, for which the centrifugal force plays a key role. Kinetic energy conservation reflects this difference: On a stably rotating spheroid, the kinetic energy is conserved in the rotating frame, whereas on a rotating sphere, it is conserved in the inertial frame. We derive these results and illustrate them using *CorioVis* software for visualizing the motion of a puck on the earth's spheroidal surface. *© 2021 Published under an exclusive license by American Association of Physics Teachers.*
https://doi.org/10.1119/10.0004801

I. INTRODUCTION

In 1679, Sir Isaac Newton and Robert Hooke discussed the possibility that the horizontal deflection of falling objects could serve as proof of the Earth's rotation; this possibility was confirmed in an 1803 measurement that agreed with calculations by Gauss and Laplace.[1] In 1835, Gaspard Gustave Coriolis showed that the total inertial force in a rotating frame is the sum of two forces, the centrifugal force and a "deflective force" that is now known as the Coriolis force.[1,2]

Despite its long history of study, the Coriolis force is a continuing source of confusion, including errors by Richard Feynman and Max Born.[3–10] The Coriolis deflection can seem downright mysterious, as anyone who has played catch with a ball on a merry-go-round can attest.[11] Students of intermediate (upper-division) classical mechanics learn how to transform Newton's second law into a uniformly rotating frame mathematically,[12] but they often cannot interpret the mathematics, appreciate the physical origins of the Coriolis and centrifugal forces, or relate them to motion as seen by an observer in the inertial frame.[13,14]

Understanding of three-dimensional latitude-dependent inertial forces for motion on a rotating planet can be particularly difficult to achieve,[15] despite the importance of these forces in meteorology,[16,17] oceanography,[18] ballistics,[19] and sniping.[20] Adding to the challenge is the lack of physical demonstrations of inertial forces for motion on a rotating sphere or spheroid.[15]

To explain why the Coriolis force deflects objects to the right in the northern hemisphere and to the left in the southern hemisphere, authors often rely on Hadley's principle.[7,16,21–25] Hadley's principle is pervasive, because it correctly predicts the direction of the Coriolis deflection for northbound and southbound motion. But Hadley's principle accounts for only half of the Coriolis deflection, includes only one of the two mechanisms responsible for this deflection, and violates conservation of angular momentum.[3]

To understand Hadley's principle, let us consider the motion of a puck that is projected directly northward from a north latitude as seen by an earthbound observer in the rotating frame (Fig. 1(a)). An inertial observer considers the puck to have two components of velocity, the northward component just discussed and an eastward component that is equal to the earth's eastward tangential velocity of rotation at that latitude (Fig. 1(d)). Hadley's principle incorrectly treats this eastward component as constant as the puck moves north, and explains Coriolis deflections by comparing the local tangential velocity of the earth's surface, which decreases as the puck moves north, with this eastward component, assumed constant.[7,21,22] The puck's eastward velocity therefore outstrips the earth's local tangential velocity, and the puck experiences a Coriolis deflection to the right as seen by an observer in the rotating frame.

The problem is that this eastward component of velocity is not constant; conservation of axial angular momentum demands that this component, as measured by an inertial observer, vary inversely with the distance from the earth's rotation axis. As the puck moves north, its distance from the earth's axis decreases and its eastward velocity *increases*. This increase accounts for the other half of the Coriolis deflection.

Many authors, some of them apparently unfamiliar with Hadley's principle, treat this eastward component of velocity as constant as an object moves toward a pole along the earth's surface,[23–25] or as an object drops vertically.[6,29–31] Such treatments violate conservation of axial angular momentum. The physics and meteorology literatures are riddled with such errors.[3,5,7,8] For both horizontal and vertical motion, conservation of axial angular momentum is needed to correctly account for Coriolis deflections.[32–34]

McIntyre[15,35] considers the motion of a puck on the surface of a uniform, spherical, frictionless, rotating earth, and he correctly applies the conservation of angular momentum. As he explains, such motion is eminently simple as viewed by an observer in the inertial frame; the puck executes
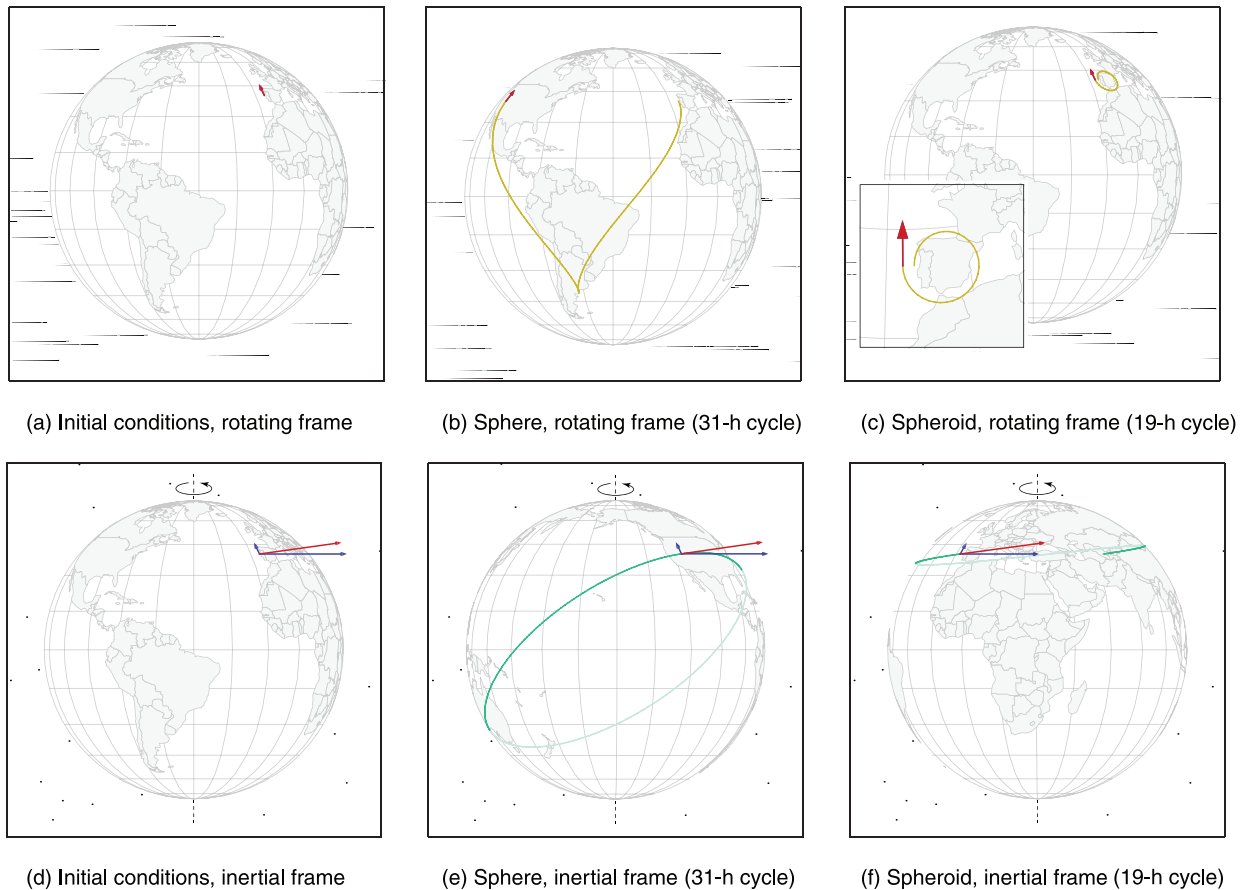
Fig. 1. *CorioVis* snapshots of one cycle of the periodic motion of a puck that slides without friction on a sphere and a stably rotating spheroid whose volumes, angular speeds of rotation, and flattening (for the spheroid) match the earth's. As viewed in the rotating frame, the puck is projected northward from latitude 40° at 50 m/s, a speed that is comparable to the fastest measured ice hockey slapshot (a) (Refs. 26 and 27). As viewed in the inertial frame, the puck's initial velocity is 360 m/s toward the northeast, including a large eastward component due to the earth's rotation (d). On the sphere (*CorioVis* (Ref. 28) Demo 1), the motion resulting from these initial conditions has period 31 h and consists of zigzag motion at a variable speed in the rotating frame (b) and motion on a great circle at a constant speed of 360 m/s in the inertial frame (e). On the spheroid (*CorioVis* (Ref. 28) Demo 2), the motion resulting from these initial conditions has period 19 h and consists of clockwise inertial oscillations at a constant speed of 50 m/s in the rotating frame (c) and incomplete orbits at a variable speed in the inertial frame (f). Blue arrows that point eastward and northward represent velocity components in these directions, and red arrows that point in the direction of motion represent velocity vectors.

uniform circular motion in a great circle around the center of the rotating sphere, visiting both the northern and southern hemispheres equally (Fig. 1(e)). As seen by an observer in the rotating frame, the puck's motion is complicated by two inertial forces, the Coriolis force and the centrifugal force (Fig. 1(b)).

The earth is not spherical, and motion on its surface differs profoundly from motion on a sphere. To see why, consider the motion of a puck that is released from rest on the surface of a frictionless spherical earth by an earthbound observer in the rotating frame. As seen by this observer, the puck experiences an unbalanced centrifugal force that drives it toward the equator. As viewed by an inertial observer, this puck has an initial eastward velocity that matches the local tangential velocity of the surface of the earth. This velocity causes the puck to drift toward the equator as the puck begins to execute a great circle around the center of the earth.

Pucks that are released from rest by earthbound observers on frictionless horizontal surfaces do not drift toward the equator, but instead remain at rest because the apparent gravitational force, defined as the vector sum of the gravitational and centrifugal forces, is everywhere perpendicular to the earth's spheroidal surface (ignoring small-scale surface features).[3] Thus, the earth's spheroidal deformations neutralize the centrifugal and gravitational forces on objects on its surface, and a puck that is released from rest in the rotating frame remains at rest. The earth's stable spheroidal shape is given by balancing the gravitational forces that hold it together against the centrifugal forces that try to tear it apart.[36]

Now let us consider the motion of a puck on the frictionless surface of this stably rotating spheroid. As seen by a rotating observer, the Coriolis force alone governs the motion of the puck, which executes "inertial oscillations" that confine it to the vicinity of its initial latitude (Fig. 1(c)).[14,37–40] Inertial oscillations have been observed in ocean currents[1] and in the atmosphere.[41,42] Unlike the great circles executed on the sphere (Fig. 1(e)), these oscillations do not generally visit both hemispheres. Clearly, motion on a stably rotating spheroid (Figs. 1(c) and 1(f)) is vastly different from motion on a sphere (Figs. 1(b) and 1(e)).

How can the motions on spherical and spheroidal earths be so different when the earth is so very nearly spherical? The earth's spheroidal deformations are small enough to be difficult to see in photographs and scale drawings, yet they are crucial to the understanding of motion on its surface. In

the geodesy literature, the relative difference between the equatorial radius a and the polar radius b of the earth is called the flattening,

$$f = \frac{a-b}{a} = 0.003353, \tag{1}$$

with the numerical value corresponding to the reference spheroid that is used in terrestrial cartography, geodesy, satellite navigation, and the global positioning system (GPS).[43–45] This reference flattening is small because of the earth's long sidereal period of rotation[43–46]

$$\tau = 23.93\,\text{h}. \tag{2}$$

The study of the effect of rotation on flattening dates back to Sir Isaac Newton, who proposed the value $f = 1/230 = 0.0043$ in his *Principia*.[47] The outlines of the earth's surface in Figs. 1(c) and 1(f) are ellipses with flattening given in Eq. (1), whereas the outlines in Figs. 1(b) and 1(e) are circles. The 0.3% difference between these outlines is virtually impossible to see, being comparable to the line width of these figures.

The earth's small flattening belies its crucial role for motion on the earth's surface, and encourages the conclusion that such motion can be well approximated by motion on a rotating sphere. This conclusion is false. Why? Because the centrifugal force plays a role for motion on a rotating sphere and does not play a role for motion on a stably rotating spheroid, whose spheroidal deformations neutralize the centrifugal and gravitational forces. The Coriolis force applies for both shapes, and its influence for motion on the earth's surface can be well approximated by treating the earth as a sphere. It is the unbalanced influence of the centrifugal force for motion on a rotating sphere that is responsible for the vast differences between this motion and motion on stably rotating spheroid. Kinetic energy conservation reflects this influence: On a stably rotating spheroid, the kinetic energy is conserved in the rotating frame, whereas on a rotating sphere, it is conserved in the inertial frame (Sec. VI).

To illustrate, we consider the forces on a 0.16-kg puck just after it is launched northward from latitude 40° at 50 m/s in the rotating frame (Fig. 1). For a rotating sphere, the gravitational and normal forces are vertical and therefore play no role in the puck's motion, which is governed in the rotating frame by a 7.5×10^{-4} N eastward Coriolis force and a 2.7×10^{-3} N southward component of the centrifugal force, which dominates the motion (Fig. 1(b)).[48] For a stably rotating spheroid, the gravitational force is no longer vertical and the puck experiences the 7.5×10^{-4} N eastward Coriolis force, the 2.7×10^{-3} N southward component of the centrifugal force, and a 2.7×10^{-3} N northward component of the gravitational force, which neutralizes the centrifugal force and leaves only the Coriolis force to govern the motion (Fig. 1(c)).[48] That the horizontal components of the gravitational and centrifugal forces cancel is no accident; it is an outcome of the balance achieved between the gravitational and centrifugal forces on a stably rotating spheroid. The large centrifugal force is unbalanced for the rotating sphere and is responsible for the vast differences between the motions on the two shapes.

Does the motion of a puck on a stably rotating spheroid replicate the motion of a puck on a *non-rotating sphere* in the limit of small angular speeds of rotation and small flattening? Yes, as long as the angular speed and the flattening obey a relationship (Sec. IV) for a stably rotating planet in hydrostatic equilibrium. This relationship predicts that a non-rotating planet is spherical. Consider a sequence of planets starting with the earth, with decreasing angular speeds and decreasing flattening that obey this relationship. At every stage in this sequence, the spheroidal deformations neutralize the centrifugal and gravitational forces, and motion on the planet's surface is governed by the Coriolis force. Being proportional to the earth's angular speed of rotation, the Coriolis force weakens with decreasing angular speed and vanishes in the limit of a non-rotating spherical planet, for which the inertial and rotating frames merge. For the 50 m/s northward launch of Fig. 1(c), as the earth's angular speed and flattening decrease, the clockwise inertial oscillations increase in amplitude until, for a non-rotating spherical planet, these oscillations are replaced by motion on a great circle that passes through both poles. Such great circles characterize motion on a sphere.[15]

Thus, a key to understanding why motion on a stably rotating spheroid differs fundamentally from motion on a rotating sphere is the realization that a rotating sphere is not in hydrostatic equilibrium, whereas a non-rotating sphere is in equilibrium.

Previous studies of motion on the spheroidal earth apply only for small flattening and assume that the earth rotates at its stable angular speed.[38,49–53] We call this the weakly spheroidal approximation.[54] To assist students in visualizing the effects of spheroidal deformations, we consider arbitrary flattening and arbitrary angular speeds of rotation.

Early in its history, the earth had a larger angular speed of rotation and therefore a larger flattening. Computer models indicate that following the astronomical impact that is thought to have created the moon, the earth's period was about 2 h.[55] This period has increased with time because lunar tidal forces convert spin angular momentum of the earth into orbital angular momentum of the moon.[13,56]

Faster-rotating planets have larger flattening than the earth. Haumea, discovered in 2004, is the third-largest dwarf planet in the solar system after Eris and Pluto.[57,58] It has flattening $f \approx 0.5$ and rotation period $\tau = 3.9$ h, the smallest of any known body in the solar system larger than 100 km.[59–61] Less extreme examples include five trans-Neptunian objects with rotation periods between 6 and 13 h.[62]

The purpose of this paper is to demonstrate the importance of the earth's spheroidal deformations for the motion of a puck on its surface, assumed smooth and frictionless. We accomplish this by discussing the applicable forces and conservation laws, illustrated with puck trajectories on spherical and spheroidal earths. Our approach is accessible to students of introductory physics and intermediate classical mechanics.

These illustrations rely on *CorioVis*, our feature-rich web-based interactive visualization software that enables students to explore the motion of a puck on an earth with arbitrary spheroidal eccentricity and arbitrary angular speed of rotation, from both the inertial and rotating frames of reference.[28,54] We offer this software freely to the physics and earth science communities to improve understanding of motion on the earth's surface.

Contributions of this paper include: (a) general treatment of motion on the spheroidal earth, (b) discussion of the role of the centrifugal force in shaping the earth and in motion on its surface, (c) consideration of conservation principles for

planets of arbitrary eccentricity that rotate at, above, and below their stable angular speeds, (d) proofs that kinetic energy is conserved in the inertial frame on a sphere and conserved in the rotating frame on a stably rotating spheroid, and (e) *CorioVis* illustrations that demonstrate the difference between motion on spherical and spheroidal earths.

The remainder of this paper is organized as follows: We review the geodetic coordinates for motion on a spheroid (Sec. II), express the Coriolis and centrifugal forces using these coordinates (Sec. III), discuss the role of the apparent gravitational force in shaping the earth (Sec. IV), prove that the axial angular momentum is conserved in the inertial frame (Sec. V), consider the conservation of kinetic energy in the inertial and rotating frames (Sec. VI), discuss puck trajectories on spherical and spheroidal earths (Sec. VII), and present brief conclusions (Sec. VIII) and acknowledgments.

See the supplementary material[48] for step-by-step details of mathematical derivations and numerical calculations in this manuscript. See also the video abstract of this manuscript.[63] Elsewhere, we derive coordinate transformations and geodetic unit vectors, model the stable angular speed of earth-like planets of arbitrary eccentricity, and present details of the development of *CorioVis* software.[54]

II. COORDINATES

We use geodetic coordinates (θ, ϕ) to describe the motion of a puck on the earth's spheroidal surface, with the geodetic latitude θ defined as the angle between the normal direction and the equatorial plane, with θ measured northward from the equator. The longitude ϕ is measured eastward from the prime meridian.[45,64] The equatorial radius a is assumed to be independent of ϕ, and the shape is an ellipsoid of revolution, called a spheroid. The geodetic latitude θ is more convenient mathematically than the geocentric latitude θ', defined as the angle between the line to the earth's center and the equatorial plane (Fig. 2). When used without qualification, the term "latitude" refers to the geodetic latitude θ, which is used for GPS coordinates and cartography.[65]

We now summarize a coordinate transformation and unit vectors that are derived elsewhere.[54] Expressed using Cartesian unit vectors $\hat{x}$, $\hat{y}$, and $\hat{z}$ that rotate with the earth, the position of the puck obeys

$$\mathbf{r} = \rho \cos \phi \, \hat{x} + \rho \sin \phi \, \hat{y} + z \hat{z}, \tag{3}$$

where

$$\rho = \frac{a \cos \theta}{\sqrt{1 - e^2 \sin^2 \theta}} \tag{4}$$

is the puck's distance from the rotation axis,

$$z = \frac{a(1 - e^2) \sin \theta}{\sqrt{1 - e^2 \sin^2 \theta}} \tag{5}$$

is its position measured northward from the equatorial plane, and

$$e = \frac{\sqrt{a^2 - b^2}}{a} \tag{6}$$

is the spheroidal eccentricity. Equation (1) yields a relationship between this eccentricity and the flattening
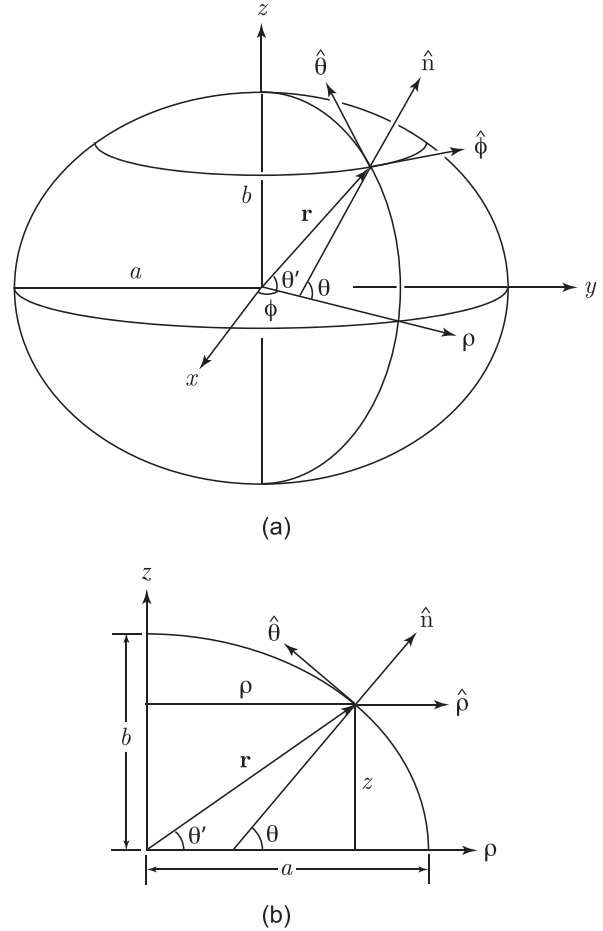

(a)

(b)

Fig. 2. Geodetic coordinates used to specify points on the surface of the earth, treated as an spheroid with equatorial radius a and polar radius b. As viewed by an observer in the rotating frame, the unit vectors $\hat{x}$, $\hat{y}$, and $\hat{z}$ are stationary, with $\hat{x}$ and $\hat{y}$ marking specific geographical points on the equator and $\hat{z}$ marking the north pole. Shown for a point on the surface are its position vector $\mathbf{r}$, its geodetic latitude θ, its geocentric latitude θ', its longitude ϕ, and its distance ρ from the axis of rotation, with orthogonal unit vectors $\hat{\phi}$, $\hat{\theta}$, and $\hat{n}$, respectively, pointing east, north, and up, and with $\hat{\rho}$ pointing away from the axis of rotation. Frame (b) shows the (ρ, z) plane of the spheroid, with $\hat{\phi}$ directed into the page.

$$e^2 = 1 - (1 - f)^2. \tag{7}$$

For spheres with $f = e = 0$, geodetic coordinates reduce to spherical coordinates.

As seen by an observer in the rotating frame, the unit vectors $\hat{x}$, $\hat{y}$, and $\hat{z}$ are stationary and point toward specific, unchanging geographical locations on the earth's surface, with $\hat{x}$ marking the intersection of the prime meridian and the equator, located off the west coast of Africa, $\hat{y}$ marking the $\phi = 90°$ east latitude position on the equator, located in the Indian Ocean, and $\hat{z}$ marking the north pole and defining the earth's rotation axis.

The unit vector

$$\hat{\rho} = \cos \phi \, \hat{x} + \sin \phi \, \hat{y} \tag{8a}$$

points from the rotation axis toward the puck and enables us to define convenient local unit vectors

$$\hat{\phi} = -\sin \phi \, \hat{x} + \cos \phi \, \hat{y}, \tag{8b}$$

$$\hat{\theta} = -\sin \theta \, \hat{\rho} + \cos \theta \, \hat{z}, \tag{8c}$$

$$\hat{n} = \cos\theta\,\hat{\rho} + \sin\theta\,\hat{z}. \qquad (8d)$$

These three vectors form a right-handed local geodetic coordinate system and, respectively, point horizontally east, horizontally north, and vertically up (Fig. 2).

III. DYNAMICS

In this section, we transform Newton's second law into the rotating frame to show the dynamical origins of the Coriolis and centrifugal forces,[12] and we express these forces using geodetic coordinates.

As seen by an observer in an inertial frame S_0, looking down from space upon the rotating spheroidal earth, a puck of mass m that slides without friction along its surface satisfies Newton's second law,

$$m\left(\frac{d^2\mathbf{r}}{dt^2}\right)_{S_0} = \mathbf{F}_g + \mathbf{F}_n, \qquad (9)$$

where

$$\mathbf{F}_g = m\mathbf{g} \qquad (10)$$

is the gravitational force on the puck, $\mathbf{g}$ is the gravitational acceleration,

$$\mathbf{F}_n = -F_n\hat{n} \qquad (11)$$

is the normal force on the puck, $\mathbf{r}$ is its position, and $(d^2\mathbf{r}/dt^2)_{S_0}$ is its acceleration as seen by an observer in the inertial frame.

We also consider the puck's motion as seen by an observer in a non-inertial frame S that rotates relative to the inertial frame with the earth's angular velocity

$$\mathbf{\Omega} = \Omega\hat{z}, \qquad (12)$$

where the angular speed

$$\Omega = \frac{2\pi}{\tau} \qquad (13)$$

follows from the earth's sidereal period τ of Eq. (2).

To transform Eq. (9) into the rotating frame, we need[12]

$$\left(\frac{d\mathbf{Q}}{dt}\right)_{S_0} = \left(\frac{d\mathbf{Q}}{dt}\right)_S + \mathbf{\Omega} \times \mathbf{Q}, \qquad (14)$$

where $(d\mathbf{Q}/dt)_{S_0}$ and $(d\mathbf{Q}/dt)_S$ are the time rates of change of a vector $\mathbf{Q}$ as observed in the inertial and rotating frames. Setting $\mathbf{Q} = \mathbf{r}$ in Eq. (14) gives a relationship between the velocities measured by the two observers

$$\left(\frac{d\mathbf{r}}{dt}\right)_{S_0} = \left(\frac{d\mathbf{r}}{dt}\right)_S + \mathbf{\Omega} \times \mathbf{r}, \qquad (15)$$

where

$$\mathbf{\Omega} \times \mathbf{r} = \Omega\rho\hat{\phi} \qquad (16)$$

is the eastward tangential velocity of the earth's rotation, obtained from Eqs. (3), (8b), and (12).[48]

Equations (3)–(5) and (8) give the puck velocity in the rotating frame (in which $\hat{x}$, $\hat{y}$, and $\hat{z}$ are stationary)[48]

$$\left(\frac{d\mathbf{r}}{dt}\right)_S = v_\phi\,\hat{\phi} + v_\theta\,\hat{\theta}, \qquad (17)$$

where

$$v_\phi = \rho\left(\frac{d\phi}{dt}\right)_S, \qquad (18a)$$

$$v_\theta = R\left(\frac{d\theta}{dt}\right)_S \qquad (18b)$$

are the associated eastward and northward components of velocity, and

$$R = \frac{(1 - e^2)a}{(1 - e^2\sin^2\theta)^{3/2}} \qquad (19)$$

is the meridional radius of curvature at latitude θ, measured along a line of longitude.[66]

Inserting Eqs. (16) and (17) into Eq. (15) gives the velocity in the inertial frame

$$\left(\frac{d\mathbf{r}}{dt}\right)_{S_0} = (\Omega\rho + v_\phi)\hat{\phi} + v_\theta\hat{\theta}, \qquad (20)$$

which includes the eastward tangential velocity $\Omega\rho\hat{\phi}$ of the earth's rotation.

Differentiating Eq. (15) and applying Eq. (14) give a relationship between the accelerations measured by observers in the two frames

$$\left(\frac{d^2\mathbf{r}}{dt^2}\right)_{S_0} = \left(\frac{d}{dt}\right)_{S_0}\left[\left(\frac{d\mathbf{r}}{dt}\right)_S + \mathbf{\Omega} \times \mathbf{r}\right] \qquad (21a)$$

$$= \left[\left(\frac{d}{dt}\right)_S + \mathbf{\Omega}\times\right]\left[\left(\frac{d\mathbf{r}}{dt}\right)_S + \mathbf{\Omega} \times \mathbf{r}\right] \qquad (21b)$$

$$= \left(\frac{d^2\mathbf{r}}{dt^2}\right)_S + 2\mathbf{\Omega} \times \left(\frac{d\mathbf{r}}{dt}\right)_S + \mathbf{\Omega} \times (\mathbf{\Omega} \times \mathbf{r}). \qquad (21c)$$

Inserting Eq. (21c) into Eq. (9) gives a modified form of Newton's second law that applies in the rotating frame

$$m\left(\frac{d^2\mathbf{r}}{dt^2}\right)_S = \mathbf{F}_g + \mathbf{F}_n + \mathbf{F}_{cor} + \mathbf{F}_{cen}, \qquad (22)$$

where the Coriolis force

$$\mathbf{F}_{cor} = -2m\mathbf{\Omega} \times \left(\frac{d\mathbf{r}}{dt}\right)_S \qquad (23)$$

and the centrifugal force

$$\mathbf{F}_{cen} = -m\mathbf{\Omega} \times (\mathbf{\Omega} \times \mathbf{r}) \qquad (24)$$

are "inertial" forces that apply only in the rotating frame. These inertial forces augment the normal and gravitational forces that also apply in the inertial frame.

The Coriolis force is perpendicular to the plane formed by the angular velocity $\mathbf{\Omega}$ of the earth and the velocity $(d\mathbf{r}/dt)_S$ of the puck as seen by an observer in the rotating frame, and applies only to objects that move relative to this observer. This force can be separated into horizontal and vertical components by combining Eqs. (8c) and (8d) to give[48]

$$\hat{\rho} = -\sin\theta\,\hat{\theta} + \cos\theta\,\hat{n} \tag{25}$$

and by invoking Eqs. (8), (12), (17), and (23),[48]

$$\mathbf{F}_{cor} = 2m\Omega\left(v_\theta\sin\theta\,\hat{\phi} + v_\phi\,\hat{\rho}\right) \tag{26a}$$

$$= 2m\Omega\sin\theta\left(v_\theta\hat{\phi} - v_\phi\hat{\theta}\right) + 2m\Omega v_\phi\cos\theta\,\hat{n} \tag{26b}$$

$$= 2m\Omega\sin\theta\left(\frac{d\mathbf{r}}{dt}\right)_S \times \hat{n} + 2m\Omega v_\phi\cos\theta\,\hat{n}. \tag{26c}$$

The horizontal component of the Coriolis force (tangent to the earth's surface) is given by the first term on the right side of Eq. (26c). This component vanishes at the equator ($\theta = 0$) and increases in magnitude with increasing $|\theta|$. This component is perpendicular to the velocity, acting to the right in the northern hemisphere ($\theta > 0$) and to the left in the southern hemisphere ($\theta < 0$). The vertical component of the Coriolis force (perpendicular to the earth's surface) is given by the second term on the right side of Eq. (26c), and is strongest near the equator.

As discussed in Sec. I, for northward motion in the rotating frame, Hadley's principle accounts for only half of the Coriolis deflection for a spherical earth.[3] To show this for the spheroidal earth, we consider a puck of mass m that is launched directly northward from a north latitude θ_0 with velocity [Eq. (17)]

$$\left(\frac{d\mathbf{r}}{dt}\right)_S = v_0\hat{\theta}, \tag{27}$$

as seen by an observer in the rotating frame. As seen by an observer in the inertial frame, the puck's initial velocity has two components, the northward component v_0 and an eastward component $\Omega\rho_0$ that matches the earth's local tangential velocity, where ρ_0 is the initial distance from the earth's rotation axis given by inserting $\theta = \theta_0$ into Eq. (4).

Hadley's principle assumes the puck's eastward velocity $\Omega\rho_0$ to be constant as it moves northward, as seen by an observer in the inertial frame, in violation of conservation of angular momentum. In the rotating frame, the associated time-dependent eastward velocity is the difference

$$v_\phi = \Omega\rho_0 - \Omega\rho \tag{28}$$

between the puck's eastward velocity $\Omega\rho_0$ in the inertial frame, assumed constant, and the earth's local tangential velocity $\Omega\rho$, which decreases as the puck moves northward. As seen by an observer in the rotating frame, the associated eastward component of force is

$$F_\phi = m\left(\frac{dv_\phi}{dt}\right)_S \tag{29a}$$

$$= m\frac{dv_\phi}{d\theta}\left(\frac{d\theta}{dt}\right)_S. \tag{29b}$$

Applying Eqs. (4), (18b), (19), and (28) and evaluating Eq. (29b) at the initial time give[48]

$$F_{\phi0} = m\Omega v_0\sin\theta_0. \tag{30}$$

This is half of the associated initial eastward Coriolis force obtained from Eq. (26b),

$$\hat{\phi}\cdot\mathbf{F}_{cor0} = 2m\Omega v_0\sin\theta_0. \tag{31}$$

Thus, Hadley's principle accounts for only half of the Coriolis deflection on a spheroid.

This result can be traced to the transformation of Newton's second law into the rotating frame. For a northward launch in the rotating frame given in Eq. (27), the initial eastward component of velocity in the inertial frame is given by the term $\mathbf{\Omega}\times\mathbf{r}$ in Eq. (15). Hadley's principle ignores the time dependence of this component, which amounts to ignoring the outer product of the expansion of Eq. (21b). The factors of 2 in Eqs. (21c) and (23) accordingly disappear, implying that Hadley's principle accounts for only half of the Coriolis deflection.

The centrifugal force applies in the rotating frame for both stationary and moving objects. Equations (8a), (8b), (12), (16), and (24) show that this force is directed away from the earth's rotation axis, according to[48]

$$\mathbf{F}_{cen} = m\Omega^2\rho\hat{\rho}. \tag{32}$$

Inserting Eq. (25) into Eq. (32) resolves the centrifugal force into horizontal and vertical components,

$$\mathbf{F}_{cen} = -m\Omega^2\rho\sin\theta\,\hat{\theta} + m\Omega^2\rho\cos\theta\,\hat{n}. \tag{33}$$

Thus, except at the poles ($\rho = 0$) and the equator ($\theta = 0$), the horizontal component of the centrifugal force drives the puck toward the equator.

IV. APPARENT GRAVITATIONAL FORCE

The gravitational and centrifugal forces do not depend on velocity, so it is natural to consider their vector sum

$$\mathbf{F}'_g = \mathbf{F}_g + \mathbf{F}_{cen}, \tag{34}$$

called the apparent gravitational force. This force plays a key role in the formation of planets. Planets can be treated as rotating self-gravitating fluid bodies that find their stable equilibrium shapes by balancing the gravitational forces that hold them together against the centrifugal forces that try to tear them apart.[36] For the hydrostatic equilibrium thus achieved, $\mathbf{F}'_g$ is perpendicular to the surface at every point on the surface.[3] Otherwise, the component of this force that is tangential to the surface will redistribute the mass of the body until this condition is achieved, in the same way that charges redistribute on the surface of a conductor in response to an applied electric field until the electric field just outside of the surface is normal to the surface.

Stable hydrostatic equilibrium establishes a relationship between the stable angular speed $\Omega = \tilde{\Omega}$ of a rotating self-gravitating fluid body and its eccentricity e. Elsewhere,[54] we model earth-like planets of arbitrary eccentricity e as MacLaurin spheroids of uniform mass density $\rho_m = 7097$ kg/m^3 and stable angular speed $\tilde{\Omega}(e)$ given by[67–71]

$$\frac{\tilde{\Omega}^2(e)}{2\pi G \rho_{\mathrm{m}}} = \frac{\sqrt{1-e^2}}{e^3}(3-2e^2)\sin^{-1}e - \frac{3}{e^2}(1-e^2), \quad (35)$$

where G is the universal gravitational constant. This model is consistent with the values

$$e = 0.08182, \qquad (36a)$$

$$\tilde{\Omega}(e) = 7.292 \times 10^{-5} \mathrm{rad/s} \qquad (36b)$$

obtained from Eqs. (1), (2), (7), and (13) for the earth's reference spheroid.[43]

We generally consider stably rotating planets with angular speeds $\Omega = \tilde{\Omega}(e)$ that coincide with their equilibrium eccentricities e. But we also find it helpful to consider $\Omega \neq \tilde{\Omega}(e)$. For this purpose, we freeze the earth into a rigid undeformable body of eccentricity e and consider the consequences of changing its angular speed.

On a stably rotating planet, the northward component of the apparent gravitational force must vanish. Accordingly, Eq. (34) gives

$$\hat{\theta} \cdot \tilde{\mathbf{F}}'_{\mathrm{g}} = \hat{\theta} \cdot \left(\mathbf{F}_{\mathrm{g}} + \tilde{\mathbf{F}}_{\mathrm{cen}}\right) = 0, \qquad (37)$$

where $\tilde{\mathbf{F}}_{\mathrm{cen}}$ and $\tilde{\mathbf{F}}'_{\mathrm{g}}$ are the centrifugal and apparent gravitational forces on the stably rotating planet. (The gravitational force $\mathbf{F}_{\mathrm{g}}$ does not depend on the rotation rate.) Combining Eq. (37) with Eqs. (10) and (33) for a stably rotating planet determines the northward component of the gravitational acceleration[48]

$$\hat{\theta} \cdot \mathbf{g} = \tilde{\Omega}^2 \rho \sin \theta, \qquad (38)$$

which vanishes at the poles and the equator. Accordingly, the gravitational acceleration can be written as

$$\mathbf{g} = -g_{\mathrm{o}}\hat{\mathrm{n}} + \tilde{\Omega}^2 \rho \sin \theta \, \hat{\theta}, \qquad (39)$$

where the first term on the right side points downward (perpendicular to the earth's surface), and the second term points horizontally toward the nearest pole. The magnitude g_{o} of the downward gravitational acceleration plays no role in the frictionless motion of a puck on the earth's surface, and we make no attempt to calculate it.

Inserting Eqs. (10), (33), and (39) into Eq. (34) gives the apparent gravitational force on a puck that moves on the surface of a planet that rotates at an arbitrary angular speed Ω,[48]

$$\mathbf{F}'_{\mathrm{g}} = m\left(-g_{\mathrm{o}} + \Omega^2 \rho \cos \theta\right)\hat{\mathrm{n}} + m\rho \sin \theta(\tilde{\Omega}^2 - \Omega^2)\hat{\theta}. \qquad (40)$$

This force is perpendicular to the surface for a stably rotating planet with $\Omega = \tilde{\Omega}(e)$.

Let us consider a puck that is released from rest on the smooth frictionless surface of the rotating earth, as seen by an observer in the rotating frame, with the puck released anywhere except the equator or the poles. Because the puck's initial velocity is zero, the initial Coriolis force on the puck is zero, and it will experience a net force given by [Eqs. (22) and (34)]

$$m\left(\frac{d^2\mathbf{r}}{dt^2}\right)_S = \mathbf{F}_{g'} + \mathbf{F}_{\mathrm{n}}, \qquad (41)$$

with $\mathbf{F}'_{\mathrm{g}}$ given in Eq. (40) and $\mathbf{F}_{\mathrm{n}}$ given in Eq. (11). If the earth rotates at its stable angular speed $\Omega = \tilde{\Omega}(e)$, the apparent gravitational force $\mathbf{F}'_{\mathrm{g}}$ is perpendicular to the earth's surface at every point on this surface, and the puck remains at rest. If $\Omega > \tilde{\Omega}(e)$, $\mathbf{F}'_{\mathrm{g}}$ has a horizontal component that drives the puck toward the equator. If $\Omega < \tilde{\Omega}(e)$, $\mathbf{F}'_{\mathrm{g}}$ has a horizontal component that drives the puck toward the nearest pole. Thus, in order for a puck to remain at rest anywhere on the earth's surface, the earth must rotate at its stable angular speed.

As seen by an observer in the inertial frame, $\mathbf{F}_{\mathrm{g}}$ and $\mathbf{F}_{\mathrm{n}}$ are the only two forces acting on a puck that slides without friction on its surface. On a *spherical* earth with $e = 0$, both forces are perpendicular to this surface and neither does any work on the puck (Fig. 3(a)), so the puck moves in uniform circular motion in a great circle around the earth's center.[15] The earth spins underneath the puck but has no effect whatsoever on its motion.

A puck that is released from rest by an observer in the rotating frame on this *spherical* earth experiences no initial Coriolis force, but does experience a centrifugal force that drives it toward the equator (Fig. 3(b)). This force tilts the apparent gravitational force away from the normal direction (Fig. 3(c)) and causes the puck to oscillate around the equator. As seen by an observer in the inertial frame, the puck has initial eastward velocity that matches the earth's local tangential velocity, and executes uniform circular motion in a great circle.

As seen by an observer in the rotating frame, a puck that is released from rest on the frictionless surface of a stably rotating *spheroidal* planet remains at rest. This is because the gravitational and centrifugal forces conspire to distribute the mass in such a way that the apparent gravitational force is perpendicular to its spheroidal surface (Fig. 3(f)). As seen by this rotating observer, the motion of a puck on the surface of such a planet is governed solely by the Coriolis force, which does no work on the puck because it is always perpendicular to its motion (Fig. 3(f)). The Coriolis force vanishes for a puck that is released from rest on this surface in the rotating frame, so this puck remains at rest.

V. ANGULAR MOMENTUM

In this section, we show that the axial angular momentum of a puck sliding along the frictionless surface of a smooth spheroidal earth is conserved in the inertial frame of reference, whether or not the earth rotates at its stable angular speed. This principle is crucial to the understanding of motion on the earth's surface, yet many treatments of such motion violate it (Sec. I).

In the inertial frame, the angular momentum of a particle of mass m is defined as

$$(\mathbf{L})_{S_0} = m\mathbf{r} \times \left(\frac{d\mathbf{r}}{dt}\right)_{S_0}. \qquad (42)$$

The axial ($\hat{z}$) component of this angular momentum is

$$(L_z)_{S_0} = m\hat{z} \cdot \left[\mathbf{r} \times \left(\frac{d\mathbf{r}}{dt}\right)_{S_0}\right]. \qquad (43)$$

As seen by an inertial observer, its time rate of change is[48]
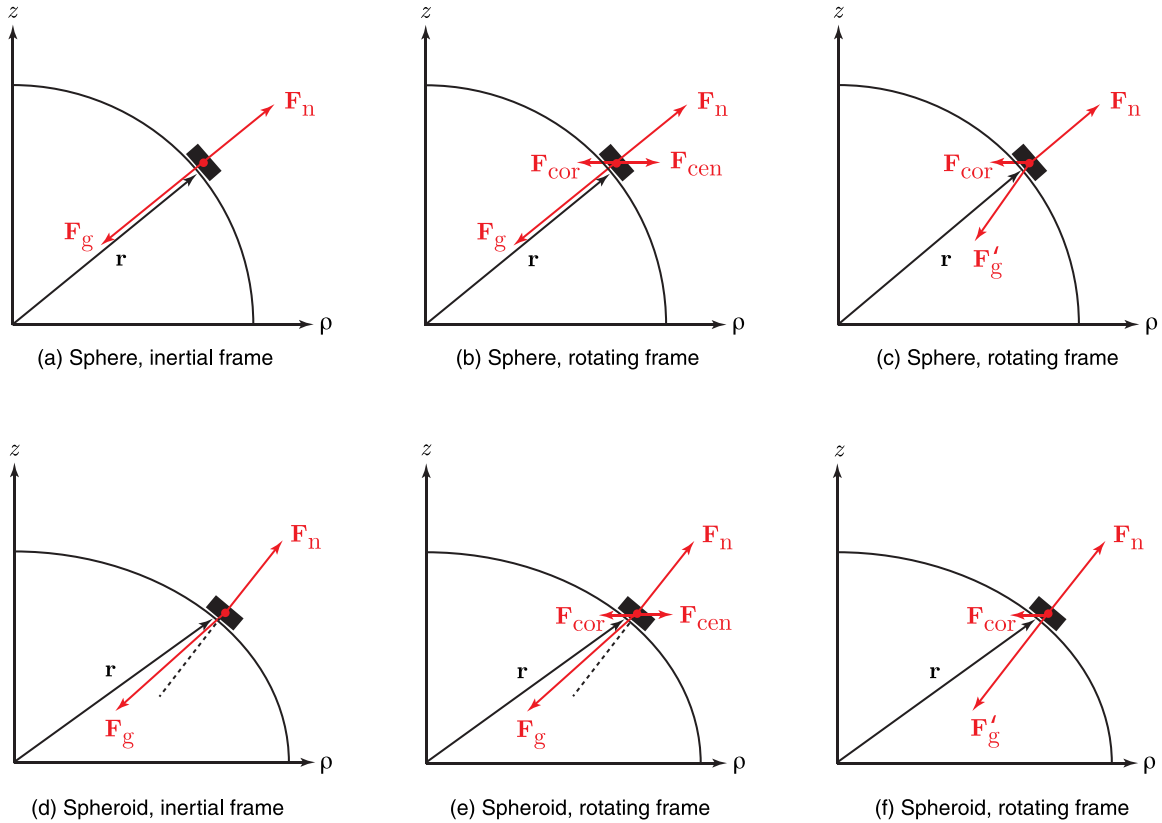
Fig. 3. Free-body diagrams showing the forces acting on a puck that slides without friction on a rotating spherical earth (a)–(c) and a stably rotating spheroidal earth ((d)–(f), with exaggerated flattening), as seen by observers in the inertial (a) and (d) and rotating (b), (c), (e), and (f) frames. Shown are the gravitational and normal forces $\mathbf{F}_g$ and $\mathbf{F}_n$ that apply in both frames; the Coriolis and centrifugal forces $\mathbf{F}_{cor}$ and $\mathbf{F}_{cen}$ that apply only in the rotating frame; and the apparent gravitational force, $\mathbf{F}'_g = \mathbf{F}_g + \mathbf{F}_{cen}$, which replaces $\mathbf{F}_g$ and $\mathbf{F}_{cen}$ in panels (c) and (f). The gravitational force $\mathbf{F}_g$ is normal to the surface of the sphere (a) and (b) and the apparent gravitational force $\mathbf{F}'_g$ is normal to the surface of the stably rotating spheroid (f). The dotted line is normal to the spheroid. The Coriolis force is zero for a stationary puck and is shown in a direction that corresponds to westward motion of the puck (directed out of the plane of the figure).

$$\frac{d}{dt}(L_z)_{S_0} = m\hat{z} \cdot \left[\mathbf{r} \times \left(\frac{d^2\mathbf{r}}{dt^2}\right)_{S_0}\right] \tag{44a}$$

$$= \left(m\frac{d^2\mathbf{r}}{dt^2}\right)_{S_0} \cdot (\hat{z} \times \mathbf{r}) \tag{44b}$$

$$= (\mathbf{F}_g + \mathbf{F}_n) \cdot \rho\hat{\phi}, \tag{44c}$$

where we have permuted the triple product in the second equality and we have used Eqs. (3), (8b), and (9) in the third. According to Eqs. (10), (11), and (39), $\mathbf{F}_g$ and $\mathbf{F}_n$ are in the (ρ, z) plane and are therefore perpendicular to $\hat{\phi}$. Hence both scalar products vanish in Eq. (44c), and[48]

$$\frac{d}{dt}(L_z)_{S_0} = 0. \tag{45}$$

Thus, *axial angular momentum is conserved in the inertial frame for motion on a frictionless spheroid, regardless of whether its angular speed of rotation matches its stable angular speed*. This result follows from Newton's second law for rotations [Eqs. (44)] and the fact that the torques exerted on the puck by the gravitational and normal forces have no components in the axial direction. The only requirement for this conservation principle is that the earth's mass be distributed symmetrically throughout the volume of a spheroid, with the normal and gravitational forces perpendicular to the eastward direction everywhere on its surface.

Permuting the triple product in Eq. (43) and invoking Eqs. (3), (8a), and (20) yield a convenient form for this conserved quantity[48]

$$(L_z)_{S_0} = m\rho(\Omega\rho + v_\phi) = \text{constant}, \tag{46}$$

where the quantity in parentheses is the eastward component of the puck velocity as seen by an observer in the inertial frame [Eq. (20)]. This eastward component is not constant, as assumed in Hadley's principle, but varies inversely with the distance ρ from the earth's rotation axis.

VI. KINETIC ENERGY

In this section, we consider the kinetic energy of a puck sliding on the frictionless surface of the spheroidal earth, as seen by an observer in the rotating frame. This kinetic energy is given by

$$(T)_S = \frac{1}{2}m\left(\frac{d\mathbf{r}}{dt}\right)^2_S, \tag{47}$$

and its time rate of change by

$$\frac{d}{dt}(T)_S = m\left(\frac{d\mathbf{r}}{dt}\right)_S \cdot \left(\frac{d^2\mathbf{r}}{dt^2}\right)_S \tag{48a}$$

$$= (\mathbf{F}_{g'} + \mathbf{F}_n + \mathbf{F}_{cor}) \cdot \left(\frac{d\mathbf{r}}{dt}\right)_S, \tag{48b}$$

where we have used Eqs. (22) and (34).

We now consider the three scalar products on the right side of Eq. (48b). The first can be rewritten using Eqs. (17) and (40),[48]

$$\mathbf{F}_{g'} \cdot \left(\frac{d\mathbf{r}}{dt}\right)_S = m(\tilde{\Omega}^2 - \Omega^2)\rho v_\theta \sin\theta. \tag{49}$$

The second vanishes through Eqs. (11) and (17), because the vectors are perpendicular[48]

$$\mathbf{F}_n \cdot \left(\frac{d\mathbf{r}}{dt}\right)_S = 0. \tag{50}$$

The third satisfies[48]

$$\mathbf{F}_{cor} \cdot \left(\frac{d\mathbf{r}}{dt}\right)_S = -2m\left[\mathbf{\Omega} \times \left(\frac{d\mathbf{r}}{dt}\right)_S\right] \cdot \left(\frac{d\mathbf{r}}{dt}\right)_S \tag{51a}$$

$$= -2m\left[\left(\frac{d\mathbf{r}}{dt}\right)_S \times \left(\frac{d\mathbf{r}}{dt}\right)_S\right] \cdot \mathbf{\Omega} \tag{51b}$$

$$= 0, \tag{51c}$$

where we have inserted Eq. (23), and we have permuted the triple product.

Combining these results with Eq. (48b) gives the time rate of change of the kinetic energy of a puck that moves without friction on the surface of a spheroidal earth, as seen by an observer in the rotating frame

$$\frac{d}{dt}(T)_S = m(\tilde{\Omega}^2 - \Omega^2)\rho v_\theta \sin\theta. \tag{52}$$

Consequently, *for spheroidal earths that rotate at the stable angular speed* $\Omega = \tilde{\Omega}$, *the puck's kinetic energy is conserved in the rotating frame*. This result follows from the work-energy theorem written in the rotating frame [Eq. (48b)]: At the stable angular speed, the apparent gravitational force, the normal force, and the Coriolis force are all perpendicular to the puck's velocity, hence none of these forces does work on the puck, and its kinetic energy is conserved. Equations (17) and (47) allow us to write this conserved quantity as[48]

$$(T)_S = \frac{1}{2}m\left(v_\phi^2 + v_\theta^2\right). \tag{53}$$

In summary, as viewed by an observer in the rotating frame, four forces act on a puck that slides without friction on the surface of a rotating planet: The gravitational force, the normal force, the Coriolis force, and the centrifugal force. If the planet is perfectly spheroidal and is rotating at its stable angular speed, then the vector sum of the gravitational and centrifugal forces, called the apparent gravitational force, is perpendicular to the planet's surface. Defining the apparent gravitational force reduces the number of forces acting on the puck to three: The apparent gravitational force, the normal force, and the Coriolis force. The apparent gravitational force and the normal force do no work on the puck, and do not change its speed, because they are directed perpendicular to its velocity. These forces do not deflect the puck, because they are directed perpendicular to the planet's surface, on which the puck is constrained to move. The Coriolis force does no

work on the puck, and does not change its speed, because this force is directed perpendicular to the puck's velocity. But the horizontal component of the Coriolis force does deflect the puck. The gravitational force and the centrifugal force each do work on the puck as it moves about on the earth's surface, but the work done by the one exactly cancels the work done by the other, and the vector sum of these forces plays no role in the motion of the puck.

A similar argument shows that *kinetic energy is conserved in the inertial frame for motion on a frictionless rotating spherical earth, regardless of its angular speed*. The corresponding conserved quantity[48]

$$(T)_{S_0} = \frac{1}{2}m\left[(\Omega\rho + v_\phi)^2 + v_\theta^2\right] \tag{54}$$

involves the square of the velocity in the inertial frame, given in Eq. (20). Evaluating the time derivative of this quantity in the inertial frame and applying Newton's second law in the inertial frame [Eq. (9)] yields two scalar products with the puck velocity in the inertial frame, both of which are zero because the normal and gravitational forces are perpendicular to the surface, hence this energy is conserved. In contrast with Eq. (53), Eq. (54) includes the earth's large tangential speed $\Omega\rho$.

The kinetic energy in the inertial frame must be conserved for frictionless motion on a spherical earth. This is because regardless of the initial position of the puck, regardless of the initial horizontal velocity of the puck (as long as it's not large enough to send the puck into orbit), and regardless of the angular speed of rotation of the earth, the puck executes uniform circular motion in great circles around the center of the earth as seen by an inertial observer, and the puck's kinetic energy in the inertial frame is therefore conserved.

This result can be confirmed using Eqs. (53) and (54),

$$(T)_{S_0} = (T)_S + \frac{m}{2}\left(\Omega^2\rho^2 + 2\Omega\rho v_\phi\right), \tag{55}$$

taking the time derivative of this result

$$\frac{d}{dt}(T)_{S_0} = \frac{d}{dt}(T)_S + \frac{m}{2}\frac{d}{dt}\left(\Omega^2\rho^2 + 2\Omega\rho v_\phi\right), \tag{56}$$

inserting Eq. (52), setting $e = \tilde{\Omega} = 0$, and comparing with the time derivative of Eq. (46) with $e = 0$, giving[48]

$$\frac{d}{dt}(T)_{S_0} = \Omega\frac{d}{dt}(L_z)_{S_0} = 0. \tag{57}$$

Because $(L_z)_{S_0}$ is a constant of the motion, $(T)_{S_0}$ is a constant of the motion, and the kinetic energy of a puck on the surface of a spherical earth is conserved in the inertial frame, regardless of the earth's angular speed.

This confirmation emphasizes the generality of Eqs. (46), (52), and (53), which govern motion on the frictionless surfaces of both spheroidal and spherical earths, whether or not they rotate at their stable angular speeds. These equations are used for our *CorioVis* software[28] because they reduce the system of coupled second-order differential equations resulting from Newton's second law to a system of coupled first-order differential equations, which are simpler to solve. *CorioVis* software is client-side and written in JAVASCRIPT, so it is available publicly for inspection.[28] Details of *CorioVis*

design, implementation, and validation are discussed elsewhere.[54]

VII. TRAJECTORIES

In this section, we use *CorioVis* visualization software to illustrate the importance of the earth's spheroidal deformations for motion on its surface,[28,54] for two sets of initial conditions. For illustrations on the spheroidal earth, we use flattening given in Eq. (1). For all illustrations, we use the earth's sidereal period of rotation given in Eq. (2) and the earth's reference equatorial radius of[43–45]

$$a = 6378.137 \, \text{km}. \tag{58}$$

A. Launch from the northern hemisphere

Figure 1 describes the motion of a puck launched off the coast of Portugal at latitude $\theta = 40°$ and longitude $\phi = -10°$, with initial northward velocity of magnitude 50 m/s as seen by an observer in the rotating frame (Fig. 1(a)). In the inertial frame, the puck's initial velocity includes a 356 m/s eastward component that matches the earth's local tangential velocity, giving the puck an initial velocity of 359 m/s toward the northeast (Fig. 1(d)). We now consider the subsequent motion of the puck on spherical and spheroidal earths, as seen in *CorioVis*[28] Demos 1 and 2.

Figure 1(b) shows the first 31-h cycle of motion of the puck on a spherical earth, as seen by an observer in the rotating frame. The puck travels from its initial latitude to its northernmost latitude of $\theta = 40.7°$, proceeds to its southernmost latitude of $\theta = -40.7°$ in Argentina, and completes its first cycle in western United States, 9000 km to the west of its initial position. The centrifugal force drives the puck toward the equator, producing a maximum puck speed of 303 m/s at equatorial crossings and a minimum speed of 7 m/s at the latitude extremes. The Coriolis force produces deflections to the right in the northern hemisphere and to the left in the southern hemisphere, which account for the puck's westward motion.

Figure 1(e) shows the first 31-h cycle of motion of the puck on a spherical earth, as seen by an observer in the inertial frame. The puck travels in a great circle around the center of the earth at a constant speed of 359 m/s, reflecting conservation of kinetic energy in the inertial frame (Sec. VI). During this time, the frictionless earth completes 1.3 rotations that have no effect on the motion of the puck.

Figure 1(c) shows the first 19-h cycle of motion of the puck on a stably rotating spheroidal earth, as seen by an observer in the rotating frame. The puck executes clockwise inertial circles between latitudes $44°$ and $35°$ at a constant speed of $v = 50$ m/s, reflecting conservation of kinetic energy in the rotating frame (Sec. VI). The puck completes its first cycle, a clockwise tour of Spain and Portugal, 170 km to the west of its initial position. Because spheroidal deformations neutralize the centrifugal and gravitational forces, the only pertinent force is the Coriolis force. According to Eq. (26c), the horizontal component of this force is perpendicular to the velocity, and has magnitude $2m\Omega v \sin|\theta|$. Setting this component equal to the product of the mass m and the centripetal acceleration v^2/r_c gives the latitude-dependent radius of curvature[14]

$$r_c = \frac{v}{2\Omega \sin|\theta|}. \tag{59}$$

As can be seen in the inset of Fig. 1(c), r_c is smallest at $\theta = 44°$, where the puck moves east, and largest at $\theta = 35°$, where the puck moves west. The puck therefore spends more time moving west than moving east, which accounts for its westward drift.[38]

Figure 1(f) shows the first 19-h cycle of motion of the puck on a stably rotating spheroidal earth, as seen by an observer in the inertial frame. The puck makes an incomplete orbit around the earth at a speed that varies between 330 m/s and 380 m/s, while the earth makes 0.8 rotations.

B. Launch from the equator

Figure 4 describes the motion of a puck launched from the equator off the west coast of Africa at latitude $\theta = 0°$ and longitude $\phi = -15°$, with initial velocity components 40 m/s westward and 30 m/s northward, giving the puck an initial velocity of 50 m/s toward the northwest, as seen in the rotating frame (Fig. 4(a)). In the inertial frame, the puck's initial velocity includes a 465 m/s eastward component that matches the earth's local tangential velocity, giving the puck an initial velocity of 426 m/s toward the northeast (Fig. 4(d)). We now consider the subsequent motion of the puck on spherical and spheroidal earths, as seen in *CorioVis*[28] Demos 3 and 4.

Figure 4(b) shows the first 26-h cycle of motion of the puck on a spherical earth, as seen in the rotating frame. The puck oscillates sinusoidally between latitudes $\pm 4°$ at a variable speed and completes its first cycle off the coast of Brazil, 3700 km to the west of its initial position. Throughout the cycle, the centrifugal and Coriolis forces oppose each other, with the centrifugal force driving the puck toward the equator and the Coriolis force driving it away, and with the centrifugal force dominating.

Figure 4(e) shows the first 26-h cycle of motion of the puck on a spherical earth, as seen in the inertial frame. The puck travels in a great circle at a constant speed of 426 m/s, reflecting conservation of kinetic energy in this frame (Sec. VI), while the frictionless earth completes 1.1 rotations.

Figure 4(c) shows the first 85-h cycle of motion of the puck on a stably rotating spheroidal earth, as seen in the rotating frame. The puck executes inertial loops between latitudes $\pm 25°$ at a constant speed of 50 m/s, reflecting conservation of kinetic energy in this frame (Sec. VI). The puck completes its first cycle 2100 km to the west of its initial position. The only pertinent force in the rotating frame is the Coriolis force, which drives clockwise loops in the northern hemisphere and counterclockwise loops in the southern hemisphere. The small horizontal components of the Coriolis force near the equator are responsible for the puck's large excursions from the equator and its long period of motion [Eq. (26c)].

Figure 4(f) shows the first 85-h cycle of motion of the puck on a stably rotating spheroidal earth, as seen in the inertial frame. The puck makes multiple orbits at a variable speed while the earth makes 3.5 rotations (Fig. 4(f)).

VIII. CONCLUSIONS

When viewed in the rotating frame, a puck that moves on the surface of a rotating sphere is subject to the centrifugal

(a) Initial conditions, rotating frame

(b) Sphere, rotating frame (26-h cycle)

(c) Spheroid, rotating frame (85-h cycle)

(d) Initial conditions, inertial frame

(e) Sphere, inertial frame (26-h cycle)
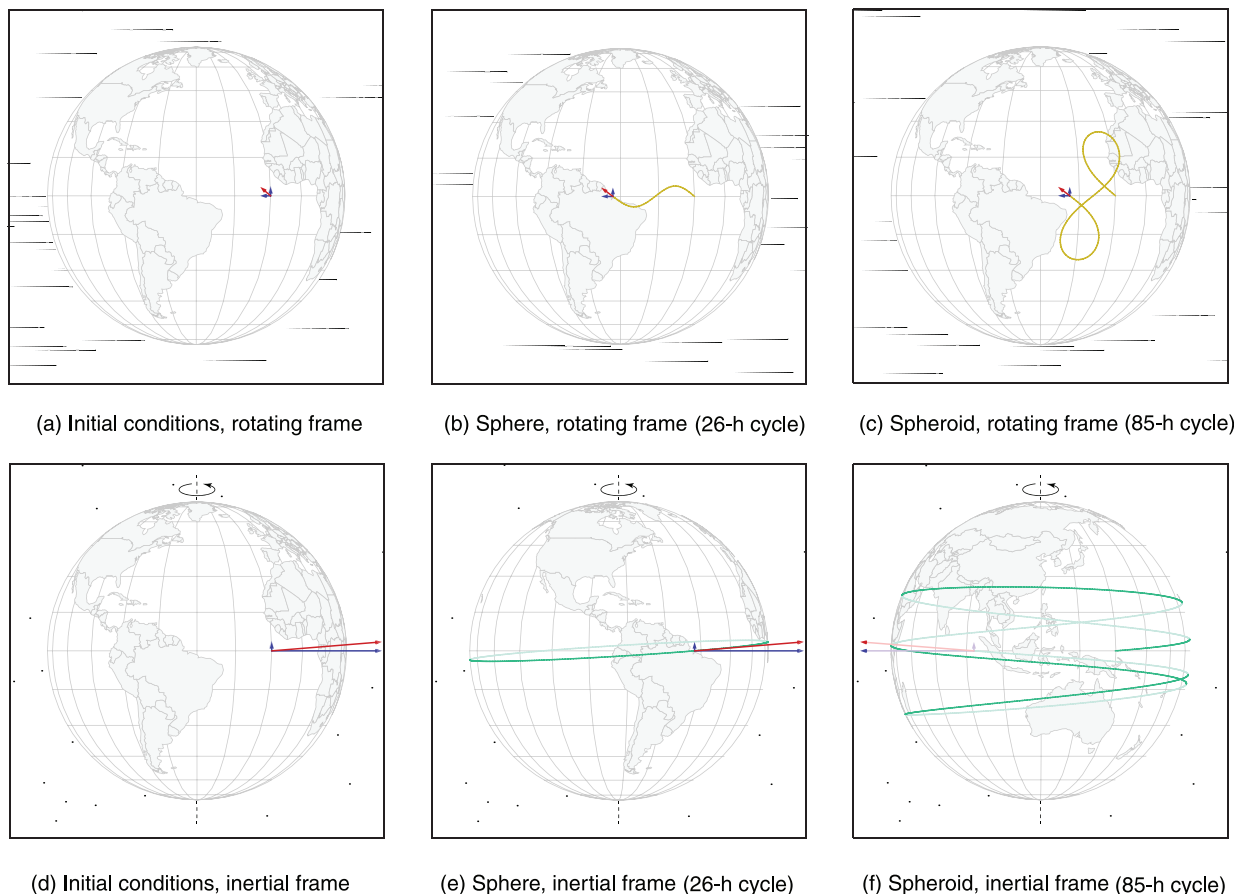
(f) Spheroid, inertial frame (85-h cycle)

Fig. 4. *CorioVis* snapshots of one cycle of the periodic motion on spherical and stably rotating spheroidal earths for a puck projected northwest from the equator at 50 m/s in the rotating frame (a). As seen by an observer in the inertial frame, the puck's initial velocity is 426 m/s toward the northeast, and includes a large eastward component due to the earth's rotation (d). On the sphere (*CorioVis* (Ref. 28) Demo 3), the motion resulting from these initial conditions has period 26 h and consists of sinusoidal motion at a variable speed in the rotating frame (b) and motion on a great circle at a constant speed of 426 m/s in the inertial frame (e). On the spheroid (*CorioVis* (Ref. 28) Demo 4), the motion resulting from these initial conditions has period 85 h and consists of inertial loops at a constant speed of 50 m/s in the rotating frame (c) and multiple orbits at a variable speed in the inertial frame (f). Blue arrows that point eastward and northward represent velocity components in these directions, and red arrows that point in the direction of motion represent velocity vectors.

force. The spheroidal deformations of a stable rotating spheroid neutralize the centrifugal and gravitational forces, so that motion on its surface bears little resemblance to motion on a sphere. Despite the basic nature of these facts and their well-known roles in meteorology and oceanography, these facts seem to be less appreciated in the physics community. This paper is designed to increase this appreciation.

Figures 1 and 4 demonstrate the importance of the earth's spheroidal deformations for two sets of initial conditions. These illustrations constitute a small subset of the wide range of possible trajectories for motion on the earth's spheroidal surface.[38,49–53]

The axial angular momentum of a puck that moves on the surface of a smooth spheroidal planet is conserved in the inertial frame (Sec. V), and its kinetic energy is conserved in the rotating frame as long as the planet rotates at its stable angular speed (Sec. VI). These conservation principles form the mathematical basis for *CorioVis*, our robust simulation and visualization software, which we offer freely to the earth science and physical science communities.[28]

We plan to use *CorioVis* to develop instructional materials to improve understanding of the origins of the earth's spheroidal deformations and the role of these deformations for motion on its surface. For this purpose, instead of using the earth's eccentricity (Figs. 1 and 4), we plan to use

exaggerated eccentricities $e \approx 0.5$ to enable students to see the earth's spheroidal deformations and to appreciate their role in the motion. *CorioVis* displays the spheroidal shape of the earth for any eccentricity (mapping the continents and graticule onto this spheroid) and is well suited for this educational purpose, especially since it also enables explorations for angular rotation speeds that are greater than, equal to, and less than the stable angular speed. We expect *CorioVis* to be useful in educating a broad spectrum of students and in dispelling long-held misconceptions about motion on the earth's surface.

Motion on planets whose angular speeds do not match their stable angular speeds, that is, motion on planets that are not in hydrostatic equilibrium, may be of interest to planetary scientists.[54] Following large collisional events, some dwarf planets may lack sufficient heat to recover hydrostatic equilibrium.[62] The moon's shape departs from hydrostatic equilibrium thanks in part to its gravitational interactions with the earth.[72] *CorioVis* may offer insights on the motion of dust or fluids on such bodies.

[a] ORCID: 0000-0002-2309-1350.

[1] A. Persson, "The Coriolis effect: Four centuries of conflict between common sense and mathematics, Part I: A history to 1885," Hist. Meteorol. **2**, 1–24 (2005), available at https://journal.meteohistory.org/index.php/hom/article/view/30.

[2] G. G. Coriolis, "Mémoire sur les équations du mouvement relatif des systèmes de corps," J. l'École Polytech. **15**, 142–154 (1835).

[3] A. Persson, "How do we understand the Coriolis force?," Bull. Am. Meteorol. Soc. **79**(7), 1373–1386 (1998).

[4] P. A. Tyvand and K. B. Haugen, "An impulsive bathtub vortex," Phys. Fluids **17**(6), 062105 (2005).

[5] M. S. Tiersten and H. Soodak, "Dropped objects and other motions relative to the noninertial earth," Am. J. Phys. **68**(2), 129–142 (2000).

[6] A. Shakur, "Debunking Coriolis force myths," Phys. Teach. **52**(8), 464–465 (2014).

[7] A. O. Persson, "Hadley's principle: Understanding and misunderstanding the trade winds," Hist. Meteorol. **3**, 17–42 (2006), available at http://meteohistory.org/2006historyofmeteorology3/2persson_hadley.pdf.

[8] M. S. Tiersten and H. Soodak, "Propagation of a Feynman error on real and inertial forces in rotating systems," Am. J. Phys. **66**(9), 810–811 (1998).

[9] J. Tessman, "Coriolis and consolation," Am. J. Phys. **55**, 392–392 (1987).

[10] J. A. Van den Akker, "Coriolis and consolation," Am. J. Phys. **55**(12), 1063 (1987).

[11] National Geographic, "Coriolis effect demonstration," <https://youtu.be/mPsLanVS1Q8> (accessed on March 18, 2021) (2021).

[12] J. R. Taylor, *Classical Mechanics* (University Science Books, Sausalito, CA, 2005), Chap. 9.

[13] A. Persson, "Mathematics versus common sense: The problem of how to communicate dynamic meteorology," Meteorol. Applicat. **17**(2), 236–242 (2010).

[14] A. Persson, "Is the Coriolis effect an 'optical illusion,'?" Q. J. R. Meteorol. Soc. **141**(690), 1957–1967 (2015).

[15] D. H. McIntyre, "Using great circles to understand motion on a rotating sphere," Am. J. Phys. **68**(12), 1097–1105 (2000).

[16] J. M. Moran, *Weather Studies: Introduction to Atmospheric Science*, 5th ed. (American Meteorological Society, Boston, MA, 2012).

[17] National Geographic, "Coriolis effect," <https://www.nationalgeographic.org/encyclopedia/coriolis-effect/> (accessed on March 18, 2021) (2021).

[18] D. Thomas and D. G. Bowers, *Introducing Oceanography* (Dunedin Academic Press Ltd., Edinburgh, 2012).

[19] O. E. Thompson, "Coriolis deflection of a ballistic projectile," Am. J. Phys. **40**(10), 1477–1483 (1972).

[20] N. Brewster, T. Kerr, N. Adams, and J. Smith, "P4_5 bending bullets," J. Phys. Spec. Top. **10**(1), 1–2 (2011), available at https://journals.le.ac.uk/ojs1/index.php/pst/article/download/2053/1956.

[21] G. Hadley, "Concerning the cause of the general trade winds," Philos. Trans. R. Soc. London **39**, 58–62 (1735).

[22] C. Abbe, *The Mechanics of the Earth's Atmosphere: A Collection of Translations* (Smithsonian Institution, Washington, DC, 1910), Vol. 51 (contains a translation of Hadley's 1735 article).

[23] J. Renault and E. Okal, "Investigating the physical nature of the Coriolis effects in the fixed frame," Am. J. Phys. **45**(7), 631–633 (1977).

[24] L. J. Battan, *Fundamentals of Meteorology*, 2nd ed. (Prentice-Hall, Englewood Cliffs, NJ, 1984).

[25] B. J. Skinner, S. C. Porter, and J. Park, *Dynamic Earth: An Introduction to Physical Geology*, 5th ed. (John Wiley & Sons, Hoboken, NJ, 2004).

[26] Guinness World Records, "Fastest ice hockey shot," <https://www.guinnessworldrecords.com/world-records/fastest-ice-hockey-shot/> (accessed on March 18, 2021) (2021).

[27] Wikipedia, "Slapshot," <https://en.wikipedia.org/wiki/Slapshot> (accessed on March 18, 2021) (2021).

[28] J. M. Edwards and B. F. Edwards, "*CorioVis* coriolis visualization software," <https://edwardsjohnmartin.github.io/coriolis/> (accessed on March 18, 2021) (2021).

[29] D. Stirling, "The eastward deflection of a falling object," Am. J. Phys. **51**(3), 236–236 (1983).

[30] E. Reddingius, "Comment on 'The eastward deflection of a falling object,'" Am. J. Phys. **52**, 562–563 (1984).

[31] D. Stirling, "Reply to 'Comment on "The eastward deflection of a falling object," ' " Am. J. Phys. **52**(6), 563 (1984).

[32] R. Bauman, "A Coriolis paradox," Phys. Teach. **21**(7), 461–462 (1983).

[33] J. Boyd and P. Raychowdhury, "Coriolis acceleration without vectors," Am. J. Phys. **49**, 498–499 (1981).

[34] P. Mohazzabi, "Free fall and angular momentum," Am. J. Phys. **67**(11), 1017–1020 (1999).

[35] D. H. McIntyre, "Coriolis force and noninertial effects animations," <http://physics.oregonstate.edu/~mcintyre/coriolis> (accessed on March 18, 2021) (2021).

[36] R. Stacey and P. Davis, *Physics of the Earth* (Cambridge U. P., Cambridge, 2008), Chap. 6.

[37] D. R. Durran, "Is the Coriolis force really responsible for the inertial oscillation?," Bull. Am. Meteorol. Soc. **74**(11), 2179–2184 (1993).

[38] P. Ripa, "Inertial' oscillations and the β-plane approximation(s)," J. Phys. Oceanogr. **27**(5), 633–647 (1997).

[39] J. R. Holton and G. J. Hakim, *An Introduction to Dynamic Meteorology* (Academic Press, Cambridge, MA, 2013).

[40] A. Wiin-Nielsen, "On inertial flow on the sphere: Technical report," <https://deepblue.lib.umich.edu/bitstream/handle/2027.42/8283/bad6752.0001.001.pdf?sequence=5&isAllowed=y> (accessed on March 18, 2021) (1973).

[41] J. Angell, "Evidence for inertial oscillations along transosonde trajectories," Mon. Weather Rev. **90**(5), 186–190 (1962).

[42] D. M. Schultz, W. E. Bracken, L. F. Bosart, G. J. Hakim, M. A. Bedrick, M. J. Dickinson, and K. R. Tyle, "The 1993 superstorm cold surge: Frontal structure, gap flow, and tropical impact," Mon. Weather Rev. **125**(1), 5–39 (1997).

[43] H. Moritz, "Geodetic reference system 1980," J. Geodesy. **74**(1), 128–133 (2000).

[44] Wikipedia, "World Geodetic System," <https://en.wikipedia.org/wiki/World_Geodetic_System#WGS84> (accessed on March 18, 2021) (2021).

[45] B. Hofmann-Wellenhof, H. Lichtenegger, and J. Collins, *Global Positioning System: Theory and Practice*, 3rd ed. (Springer-Verlag, New York, 1994).

[46] The pertinent period of rotation is the sidereal period of rotation given in Eq. (2), which is the time required for the earth to spin once on its axis relative to the fixed stars. This period differs slightly from the mean solar day of 24 h, the average time required for the earth to spin once on its axis relative to the sun. The mean solar day is longer than the sidereal period because of the earth's orbital motion around the sun, which is in the same direction as the earth's spin.

[47] A. Motte, *Translation of Newton's Principia (1687), Axioms or Laws of Motion* (Daniel Adee, New York, 1846), Book III, Proposition XIX, Problem III, pp. 405–408 <https://archive.org/details/newtonspmathema00newtrich>.

[48] See supplementary material at https://www.scitation.org/doi/suppl/10.1119/10.0004801 with step-by-step details of mathematical derivations and numerical calculations in this manuscript.

[49] P. Ripa, "Effects of the earth's curvature on the dynamics of isolated objects. Part I: The disk," J. Phys. Oceanogr. **30**(8), 2072–2087 (2000).

[50] P. Ripa, "Effects of the earth's curvature on the dynamics of isolated objects. Part II: The uniformly translating vortex," J. Phys. Oceanogr. **30**(10), 2504–2514 (2000).

[51] N. Paldor and P. D. Killworth, "Inertial trajectories on a rotating earth," J. Atmos. Sci. **45**(24), 4013–4019 (1988).

[52] N. Paldor and A. Sigalov, "The mechanics of inertial motion on the earth and on a rotating sphere," Phys. D: Nonlinear Phenom. **160**, 29–53 (2001).

[53] J. J. Early, "The forces of inertial oscillations," Q. J. R. Meteorol. Soc. **138**(668), 1914–1922 (2012).

[54] B. F. Edwards and J. M. Edwards, "Geodetic model for teaching motion on the earth's spheroidal surface," Eur. J. Phys. (in press) (2021).

[55] M. Cuk and S. T. Stewart, "Making the moon from a fast-spinning earth: A giant impact followed by resonant despinning," Science **338**(6110), 1047–1052 (2012).

[56] W. Peltier, "The history of the earth's rotation: Impacts of deep earth physics and surface climate variability," in *Treatise on Geophysics*,

2nd ed., edited by Gerald Schubert (Elsevier, Oxford, 2015), Chap. 9.09, pp. 221–279.

[57]D. Ragozzine and M. E. Brown, "Orbits and masses of the satellites of the dwarf planet Haumea (2003 EL61)," Astronom. J. **137**(6), 4766–4776 (2009).

[58]Wikipedia, "Dwarf planet," <https://en.wikipedia.org/wiki/Dwarf_planet> (accessed on March 18, 2021) (2021).

[59]D. L. Rabinowitz, K. Barkume, M. E. Brown, H. Roe, M. Schwartz, S. Tourtellotte, and C. Trujillo, "Photometric observations constraining the size, shape, and albedo of 2003 EL61, a rapidly rotating, Pluto-sized object in the Kuiper belt," Astrophys. J. **639**(2), 1238–1251 (2006).

[60]L. Christensen, "IAU names fifth dwarf planet Haumea," <https://www.iau.org/news/pressreleases/detail/iau0807/> (accessed on March 18, 2021) (2008).

[61]J. L. Ortiz, P. Santos-Sanz, B. Sicardy, G. Benedetti-Rossi, D. Bérard, N. Morales, R. Duffard, F. Braga-Ribas, U. Hopp, C. Ries *et al.*, "The size, shape, density and ring of the dwarf planet Haumea from a stellar occultation," Nature **550**(7675), 219–223 (2017).

[62]N. Rambaux, D. Baguet, F. Chambat, and J. C. Castillo-Rogez, "Equilibrium shapes of large trans-Neptunian objects," Astrophys. J. Lett. **850**(1), L9–L13 (2017).

[63]Video abstract of this manuscript, see https://doi.org/10.1119/10.0004801.

[64]Wikipedia, "Geographic coordinate conversion," <https://en.wikipedia.org/wiki/Geographic_coordinate_conversion> (accessed on March 18, 2021) (2021).

[65]Wikipedia, "Latitude," <https://en.wikipedia.org/wiki/Latitude> (accessed on March 18, 2021) (2021).

[66]Wikipedia, "Earth radius," <https://en.wikipedia.org/wiki/Earth_radius> (accessed on March 18, 2021) (2021).

[67]C. MacLaurin, *A Treatise of Fluxions: In Two Books* (Ruddimans, Edinburgh, 1742), Vol. 1.

[68]S. Chandrasekhar, *Ellipsoidal Figures of Equilibrium* (Yale U. P., London, 1969).

[69]R. Lyttleton, *The Stability of Rotating Liquid Masses* (Cambridge U. P., Cambridge, 1953).

[70]Wikipedia, "Maclaurin spheroid," <https://en.wikipedia.org/wiki/Maclaurin_spheroid> (accessed on March 18, 2021) (2021).

[71]E. Poisson and C. M. Will, *Gravity: Newtonian, Post-Newtonian, Relativistic* (Cambridge U. P., Cambridge, 2014).

[72]S. Runcorn and M. Shrubsall, "The figure of the moon," Phys. Earth Planet. Inter. **1**(5), 317–325 (1968).
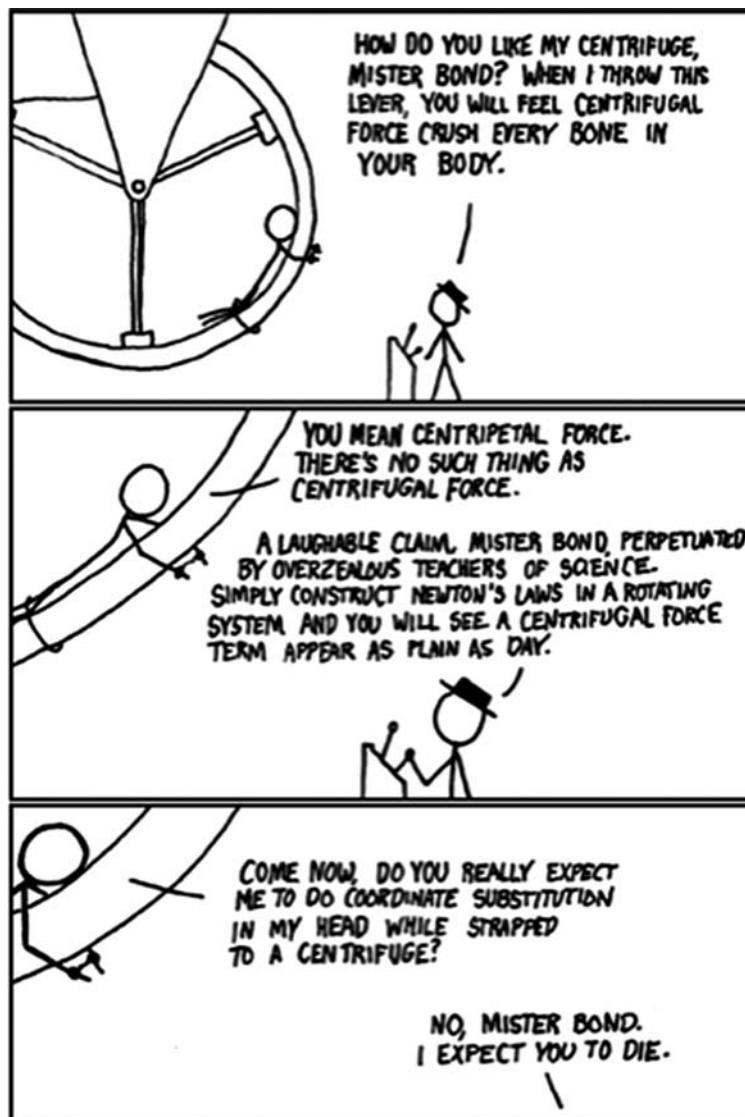
CENTRIFUGAL FORCE

You spin me right round baby, right round, in a manner depriving me of an inertial reference frame. Baby. (Source: https://xkcd.com/123/)